WARWICK
THE UNIVERSITY OF WARWICK

Manuscript version: Author's Accepted Manuscript
The version presented in WRAP is the author's accepted manuscript and may differ from the published version or Version of Record.

Persistent WRAP URL:
http://wrap.warwick.ac.uk/136528

How to cite:
Please refer to published version for the most recent bibliographic citation information. If a published version is known of, the repository item page linked to above, will contain details on accessing it.

Copyright and reuse:
The Warwick Research Archive Portal (WRAP) makes this work by researchers of the University of Warwick available open access under the following conditions.

Copyright © and all moral rights to the version of the paper presented here belong to the individual author(s) and/or other copyright owners. To the extent reasonable and practicable the material made available in WRAP has been checked for eligibility before being made available.

Copies of full items can be used for personal research or study, educational, or not-for-profit purposes without prior permission or charge. Provided that the authors, title and full bibliographic details are credited, a hyperlink and/or URL is given for the original metadata page and the content is not changed in any way.

Publisher's statement:
Please refer to the repository item page, publisher's statement section, for further information.

For more information, please contact the WRAP Team at: wrap@warwick.ac.uk.

warwick.ac.uk/lib-publications

Modulation Parameter Estimation of LFM Interference for Direct Sequence Spread Spectrum Communication System in Alpha-Stable Noise

Mingqian Liu, *Member, IEEE,* Yuting Han, Yunfei Chen, *Senior Member, IEEE,* Hao Song, Zhutian Yang, *Senior Member, IEEE,* and Fengkui Gong, *Member, IEEE*

***Abstract*—The linear frequency modulation (LFM) interference is one of the typical broadband interferences in direct sequence spread spectrum (DSSS) communication system. In this paper, a novel modulation parameter estimation method of LFM interference is proposed for DSSS communication system in alpha-stable noise. To accurately estimate the modulation parameters, the alpha-stable noise should be eliminated first. Thus, we formulate a new generalized extended linear chirplet transform (GELCT) to suppress the alpha-stable noise, for a robust time-frequency transformation of LFM interference is realized. Then, using the Radon transform, the maximum value after transformation and the chirp rate according to the angle related to the maximum value are estimated. In addition, a generalized Fourier transform (GFT) is introduced to estimate the initial frequency of the LFM interference. For performance analysis, the Cramér-Rao lower bounds of the estimated chirp rate and the initial frequency of the LFM interference in the presence of alpha-stable noise are derived. Moreover, the asymptotic properties of the modulation parameter estimator are analyzed. Simulation results demonstrate that the performance of the proposed parameter estimation method significantly outperforms existing methods, especially in a low SNR regime.**

***Index Terms*—Alpha-stable noise, Cramér-Rao lower bound, generalized extended linear chirplet transform, generalized Fourier transform, linear frequency modulation, parameter estimation.**

I. Introduction

LINEAR frequency modulation (LFM) occupies a wide bandwidth to offer a high system processing gain. Due to this attribute, LFM have been widely used in wireless communications, radar, and sonar systems [1]. Due to the wide applications of LFM, wireless communication systems, such as direct sequence spread spectrum (DSSS) communication systems, may suffer from the interference caused by LFM interference, which can be characterized as a common broadband non-stationary interference. To effectively reduce the interference, the parameters of LFM interference should be accurately estimated, so that the interference caused by LFM to DSSS systems can be characterized and countered to provide a frequency modulation scheme with a high interference suppressing ability. Thus, parameter estimation of LFM interference is very critical for DSSS communication systems. LFM interference could be defined as the interference with linearly time-varying instantaneous frequency. There are two basic parameters, the chirp rate and the initial frequency, that describe the instantaneous frequency of LFM interference. Therefore, this paper aims to estimate the chirp rate and the initial frequency of the LFM interference.After estimating the modulation parameters of the LFM interference, a demodulation reference signal can be constructed, and the interference term becomes a single frequency component, so that the interference term can be suppressed by a notch filter [2]. Nowadays, in the context of Industry 4.0, interference detection and suspicious identification in industrial equipments are required to be intelligent [3]. Interference parameters estimation can be used as prior information to lay the foundation for its intelligent implementation.

The interferences of DSSS system are divided into narrowband interference and broadband interference. The narrowband interference suppression methods include time domain adaptive processing and transform domain processing. Transform-domain interference suppression technologies include Fourier transform, wavelet transform, and overlapping transform. At present, the proposed broadband interference suppression methods include compressed sensing algorithm [4], Wigner-Ville distribution and Hough transform (WHT) algorithm [2], fractional Fourier transform algorithm [5], and so on. However, when the interference power is low, there is an error in the time-frequency analysis, and the parameters of the interference signal cannot be accurately estimated, so that its suppression performance is degraded. The method for estimating the interference parameters is better in the suppression effect, which makes the bit error rate at the receiving end lower. Therefore, the interference can be analyzed and processed in depth through the estimated interference parameters, so as to design an interference suppression method with better performance.

This work was supported by the National Natural Science Foundation of China under Grant 61501348 and 61801363, Shaanxi Provincial Key Research and Development Program under Grant 2019GY-043, Joint Fund of Ministry of Education of the People's Republic of China under Grant 6141A02022338, China Postdoctoral Science Foundation under Grant 2017M611912, the 111 Project under Grant B08038 and the China Scholarship Council under Grant 201806965031. *(Corresponding author: Yuting Han.)*

M. Liu, Y. Han and F. Gong are with the State Key Laboratory of Integrated Service Networks, Xidian University, Shaanxi, Xi'an 710071, China (e-mail: mqliu@mail.xidian.edu.cn; hytxidian@163.com; fkgong@xidian.edu.cn).

Y. Chen is with the School of Engineering, University of Warwick, Coventry, West Midlands United Kingdom of Great Britain and Northern Ireland CV4 7AL (e-mail: yunfei.chen@warwick.ac.uk).

H. Song is with the Bradley Department of Electrical and Computer Engineering, Virginia Tech, Blacksburg, VA 24060, USA (e-mail: haosong@vt.edu).

Z. Yang is with the School of Electronics and Information Engineering, Harbin Institute of Technology, Harbin 150001, China (e-mail: yangzhutian@hit.edu.cn).

In wireless communications, frequency multiplexing is commonly used to enhance system capacity. However, due to the reuse of frequency resource, co-channel interference arises [6]. As a result, environmental noise in wireless communications has strong randomness and impulsiveness [7]. To precisely model such a wireless environment, alpha-stable distribution is commonly used. Alpha-stable distribution captures the bursty characteristics of the pulse in a real wireless environment. Hence, in this paper, we focus on studying the modulation parameter estimation of LFM interference in the alpha-stable noise.

The parameter estimation of LFM interference has been widely studied. In [8], the fractional Fourier transform was used to estimate the chirp rate of the LFM interference. However, this method requires two-dimensional search with high complexity. In [9], the parameters of LFM interference were estimated by using the modulus fractional cross-spectrum and cubic spline interpolation. In [10], short-time Fourier transform (STFT) was used to approximate the local signal to a stationary signal by adding windows. In [11], a LFM modulation parameter estimation method based on STFT transform was proposed. The STFT used a long window length to enhance LFM interference. Then, frequency shift and energy accumulation according to STFT results were obtained, and the chirp rate was roughly estimated. Finally, a fine search of the chirp rate was carried out by using a suitable short window length and search step size to accurately estimate the parameters. In [12], a new method was proposed to shorten the estimation time. Unfortunately, all these methods cannot be adapted to LFM interference in alpha-stable noise, thus making the parameter estimation of LFM interference more challenging.

To estimate the parameters of LFM interference in the alpha-stable noise environment, a method based on fractional Fourier transform and Sigmoid transform was proposed in [13]. Although this method can be used in the impulse noise environment and effectively estimated the parameters of LFM interference, the estimation performance degrades significantly in the low SNR regime. In [14], a combination of fractional lower-order statistics and scaled ambiguity transformation was introduced to improve the performance of impulse noise environments and estimated the modulation parameters of LFM interference. However, the estimation error of this method was large. In [15], a fractional low-order covariance (FLOC) fractional spectrum estimation algorithm was proposed to estimate the LFM interference parameters. However, according to the experimental results presented, the overall error was large and the estimation performance was not satisfaction. In [16], the impulse noise was suppressed by using the nonlinear transformation. Then, the fractional Fourier transform (FRFT) was used to identify the LFM interference and the parameters are roughly estimated according to the peak coordinates. Finally, a two-dimensional particle swarm optimization (PSO) algorithm was used to estimate the parameters. However, this method had a high computational complexity.

In this paper, to further improve the accuracy in alpha-stable noise, especially in a low SNR regime, a novel method is proposed using a generalized extended linear chirplet transform (GELCT) and a generalized Fourier transform (GFT) to estimate modulation parameters of LFM interference for DSSS communication system. The main creative contributions of this paper can be summarized as follows:

- In order to accurately estimate the modulation parameters of LFM interference, the GELCT-Radon transform is used to estimate the chirp rate. More specifically, the GELCT transform applies nonlinear transformation to the signal first to suppress the alpha-stable noise, and then carries out time-frequency transformation. On the other hand, the Radon transform converts a two-dimensional plane function into a linear function defined in two-dimensional space. The line on the GELCT plane is integrated, and a peak point is achieved on the new plane. After searching for the peak, the chirp rate of the signal can be estimated.
- For the estimation of the initial frequency, a GFT method is proposed, which is used to suppress the alpha-stable noise and convert the signal from the time domain to the frequency domain. Then, the initial frequency is effectively and accurately estimated.
- The asymptotic property of the chirp rate and the initial frequency estimator is thoroughly analyzed to show that the proposed method is asymptotically consistent.
- The Cramér-Rao lower bounds (CRLBs) of the modulation parameter estimation of LFM interference in alpha-stable noise are derived. A lower bound is analyzed for the variance of the unbiased estimator.

The remainder of the paper is organized as follows. The signal and noise models are presented in Section II. Section III describes the proposed algorithm for joint estimations of modulation parameters of LFM interference. Section IV illustrates the asymptotic property of the modulation parameters estimator. In Section V, the CRLBs for the estimation of LFM interference' modulation parameters are derived in alpha-stable noise. The simulation results are given in Section VI. Finally, conclusions are made in Section VII.

II. System Model

DSSS communication system that encounter LFM interference will be considered in this paper, where the receive signal of the DSSS system in interference condition can be given by

$$r(t) = x(t) + s(t) + e(t), \tag{1}$$

where $x(t)$ represents the useful communication signal, $s(t)$ is the LFM interference, $e(t)$ is the alpha-stable noise, and $s(t)$ is expressed as

$$s(t) = A\exp(j2\pi f_0 t + j\pi k t^2), \tag{2}$$

where A is the signal amplitude, f_0 is the initial frequency, k is the chirp rate, which is the ratio of the modulation bandwidth to the pulse bandwidth. The instantaneous phase of the signal is $\phi(t) = 2\pi f_0 t + \pi k t^2$ and the instantaneous frequency is $f(t) = f_0 + kt$. The probability density function (P.D.F.) of the alpha-stable random variable has no closed form, thus $e(t)$ is expressed by the characteristic function as [17]

$$\varphi(t) = \exp\{j\delta t - \gamma|t|^{\alpha}[1 + j\beta\mathrm{sgn}(t)w(t,\alpha)]\}, \tag{3}$$

where

$$\mathrm{sgn}(t) = \begin{cases} 1, t > 0, \\ 0, t = 0, \\ -1, t < 0, \end{cases} \tag{4}$$

$$w(t,\alpha) = \begin{cases} \tan(\alpha\pi/2), \alpha \neq 1, \\ (2/\pi)\log|t|, \alpha = 1. \end{cases} \tag{5}$$

The parameters in (3) are:

- α is the characteristic exponent with $0 < \alpha \leq 2$, which determines the shape of the stable distribution or the heaviness of the tail of the stable density. When $\alpha = 2$, (3) corresponds to the characteristic function of a Gaussian distribution with variance 2γ.
- γ is the dispersion parameter with $\gamma \geq 0$, and is similar to the variance of Gaussian noise, which determines the spread of the distribution around the center.
- β is the index of skewness with $-1 \leq \beta \leq 1$, which controls the symmetry of the distribution.
- δ is the location parameter, which indicates the center of the P.D.F. of the alpha-stable distribution on the x-axis, and the value interval is the real number field.

This paper uses the symmetric alpha-stable ($S\alpha S$) distribution, i. e. both the index of skewness β and the location parameter δ are 0, and the dispersion parameter γ assumed as 1. Also, we assume the characteristic exponent α has a value range of $1 \leq \alpha \leq 2$.

Since the finite second-order statistical moment of $S\alpha S$ noise does not exist, the signal-to-noise ratio (SNR) in the traditional sense is redefined based on the dispersion coefficient γ of the alpha-stable noise and the variance of the signal σ_s^2 as the generalized SNR (GSNR), which can be defined as

$$GSNR = 10\log_{10}(\sigma_s^2/\gamma). \tag{6}$$

III. Joint Modulation Parameter Estimation of LFM Interference

A. Chirp Rate Estimation

The chirplet transform can extract a number of frequency components from a certain type of signal [18]-[20]. Hence, this transform can be used to estimate the chirp rate. Since $S\alpha S$ noise does not have second and higher-order statistics, this paper proposes a generalized extended linear Chirplet transform (GELCT), which is expressed as

$$G(t,w) = \int_{-\infty}^{\infty} f[r(\tau)]h(\tau - t)e^{-jw\tau}e^{-j\frac{1}{2}(\tau-t)^2\frac{f_s}{2T_s}\tan\vartheta}d\tau, \tag{7}$$

where $r(\tau)$ is the received signal, $h(\cdot)$ is the window function, f_s is the sampling frequency, T_s is the sampling time, and $\vartheta = -\pi/2 + l\pi/(L+1), l = 1, 2, \cdots, L$. In addition, $f[\cdot]$ is the nonlinear transformation, expressed as

$$f[r(t)] = \left(\frac{\log_e(|r(t)|)^{\frac{1}{e}} + 1}{|r(t)|}\right) r(t), |r(t)| \neq 0. \tag{8}$$

From (7), it is clear that the GELCT is applied to the signals by nonlinear transformation to suppress the alpha-stable noise, and then performs a chirplet transform. From (8), it is observed that the nonlinear transformation of the received signal with $S\alpha S$ noise can limit the infinite amplitude of the noise to a limited range, so as to existence of the second and higher-order statistics, while retaining useful information about the signal. Therefore, the statistics above the second order can still play their role.

Property 1: The nonlinear transformation defined in (8) maps the amplitude of the signal to a finite range. For signals in $S\alpha S$ noise, the amplitude of the noise is also mapped to this range without changing the period and phase information of the signal.

Proof: See Appendix A. ∎

The Radon transform is applied to the line detection in the time-frequency domain after the GELCT is applied to estimate the parameters of the signal [21]. The procedures of the Radon transform are to rotate the time-frequency right-angle coordinate (t, w) of the original time-frequency domain by v angles to obtain a new angular radius coordinate (u, v), and to integrate the line with different u parallel to the v-axis. The Radon transform actually maps any line on plane (t, w) to a point on plane (u, v), and each point (u_0, v_0) on plane (u, v) determines a line equation $t\cos v_0 + w\sin v_0 = u_0$.

For the time-frequency analysis graph $G(t, w)$, the Radon transform is given by

$$R(u,v) = \int_L G(t,w)ds, \tag{9}$$

where ds is the line micro-element on L, the equation of the straight line L is $t\cos v + w\sin v = u$. The Delta function is a generalized function that the function takes a value of 0 at non-zero points, and the integral in the entire domain is 1. It is expressed as

$$\delta(x) = \begin{cases} 0, x \neq 0, \\ 1, x = 0. \end{cases} \tag{10}$$

According to the equation of a line, the Delta function can be expressed as

$$\delta(t\cos v + w\sin v - u) = \begin{cases} 0, t\cos v + w\sin v - u \neq 0, \\ 1, t\cos v + w\sin v - u = 0. \end{cases} \tag{11}$$

The point (t, w) on the time-frequency analysis graph $G(t, w)$ satisfies $\delta(x) = 1$, and the points on the other non-time-frequency analysis graph $G(t, w)$ satisfy $\delta(x) = 0$. Thus, the Radon transform becomes

$$R(u,v) = \int_{-\infty}^{\infty}\int_{-\infty}^{\infty} G(t,w)\delta(t\cos v + w\sin v - u)dtdw. \tag{12}$$

The GELCT has the effect of compressing and focusing the LFM signal, which can suppress the influence of $S\alpha S$ noise to some extent. The Radon transform can integrate the line on the GELCT plane and integrate it into a peak point on the (u, v) plane. By searching for the peak, according to $\hat{k} = -\cot(\hat{v})$, we can estimate the chirp rate $\hat{k}$ of the signal. The peak of the Radon transform can be expressed as

$$R_{\max}(\hat{u},\hat{v}) = \max_{u,v}[R(u,v)]. \tag{13}$$

Therefore, the chirp rate of the LFM interference is estimated as

$$\hat{k} = -\cot(\hat{v})\Delta f/\Delta t, \tag{14}$$

where Δf and Δt are the frequency-domain sampling interval and the time-domain sampling interval of the GELCT, respectively.

The procedure of the chirp rate estimation for LFM interference in $S\alpha S$ noise is summarized in Algorithm 1.

Algorithm 1 The chirp rate estimation for LFM interference in $S\alpha S$ noise

Input: $r(t)$: the received signal.

Output: $\hat{k}$: the estimated value of the chirp rate.

1: Perform GELCT time-frequency analysis on the received signal by $G(t,w) = \int_{-\infty}^{\infty} f[r(\tau)]h(\tau-t)e^{-jw\tau}e^{-j\frac{1}{2}(\tau-t)^2\frac{f_s}{2T_s}\tan\vartheta}d\tau$;

2: The time-frequency analysis graph $G(t,w)$ is Radon transformed to obtain $R(u,v)$ by $R(u,v) = \int_L G(t,w)ds$;

3: Obtain the maximum value $R_{\max}(\hat{u},\hat{v})$ of $R(u,v)$ by $R_{\max}(\hat{u},\hat{v}) = \max_{u,v}[R(u,v)]$;

4: Estimate the chirp rate $\hat{k}$ according to the angle $\hat{v}$ corresponding to the maximum value by $\hat{k} = -\cot(\hat{v})\Delta f/\Delta t$.

B. Initial Frequency Estimation

When estimating the initial frequency, the demodulation reference signal $e^{-j\pi\hat{k}t^2}$ is constructed by using the estimated chirp rate $\hat{k}$. Multiplied by the received signal $r(t)$, $r_1(t)$ is obtained as

$$\begin{aligned} r_1(t) &= (x(t)+s(t)+e(t))\,e^{-j\pi\hat{k}t^2} \\ &= x(t)\cdot e^{-j\pi\hat{k}t^2} + Ae^{j2\pi f_0 t + j\pi k t^2}\cdot e^{-j\pi\hat{k}t^2} \\ &\quad + e(t)\cdot e^{-j\pi\hat{k}t^2} \\ &= x(t)\cdot e^{-j\pi\hat{k}t^2} + Ae^{j2\pi f_0 t} + e(t)\cdot e^{-j\pi\hat{k}t^2}. \end{aligned} \tag{15}$$

After obtaining the signal $r_1(t)$, GFT is performed to convert the signal from the time domain to the frequency domain, thereby extracting the information of the initial frequency in $r_1(t)$. In this paper, we propose GFT which is based on performing a nonlinear transformation as shown in (8) on the signal, and then performing a Fourier transform as follows

$$GF(w) = \int_{-\infty}^{\infty} f[r_1(t)]e^{-jwt}dt \tag{16}$$

Property 2: Nonlinear transformation on $r_1(t)$ can suppress alpha-stable noise and preserve useful information of the signal.

Proof: See Appendix B. ∎

According to property 2, (16) can be expressed as follows:

$$\begin{aligned} GF(w) &= \int_{-\infty}^{\infty} f[r_1(t)]e^{-jwt}dt \\ &= \int_{-\infty}^{\infty} (x_1(t)+s_1(t)+e_1(t))e^{-jwt}dt \\ &= \int_{-\infty}^{\infty} s_1(t)e^{-jwt}dt + \int_{-\infty}^{\infty}(x_1(t)+e_1(t))e^{-jwt}dt \\ &= \int_{-\infty}^{\infty} c(t)Ae^{j2\pi f_0 t}e^{-jwt}dt \\ &\quad + \int_{-\infty}^{\infty} c(t)(x(t)+e(t))e^{-j\pi\hat{k}t^2}e^{-jwt}dt \end{aligned} \tag{17}$$

where $c(t) = \frac{\log_e(|x(t)+A+e(t)|)^{\frac{1}{e}}+1}{|x(t)+A+e(t)|}$, when the noise is low, $c(t) \approx \frac{\log_e(|x(t)+A|)^{\frac{1}{e}}+1}{|x(t)+A|}$. Thus, (17) can be rewritten as:

$$\begin{aligned} GF(w) &= \int_{-\infty}^{\infty} c(t)Ae^{j2\pi f_0 t}e^{-jwt}dt \\ &\quad + \int_{-\infty}^{\infty} c(t)(x(t)+e(t))e^{-j\pi\hat{k}t^2}e^{-jwt}dt \\ &\approx \int_{-\infty}^{\infty} \frac{\log_e(|x(t)+A|)^{\frac{1}{e}}+1}{|x(t)+A|}Ae^{j2\pi f_0 t}e^{-jwt}dt \\ &\quad + \int_{-\infty}^{\infty} c(t)(x(t)+e(t))e^{-j\pi\hat{k}t^2}e^{-jwt}dt \\ &\approx A\left(\frac{\log_e(|x(t)+A|)^{\frac{1}{e}}+1}{|x(t)+A|}\right)\int_{-\infty}^{\infty} e^{j2\pi f_0 t}e^{-jwt}dt \\ &\quad + N(w) \\ &\approx A\left(\frac{\log_e(|x(t)+A|)^{\frac{1}{e}}+1}{|x(t)+A|}\right)\delta(w-2\pi f_0) \\ &\quad + N(w) \end{aligned} \tag{18}$$

where $N(w) = \int_{-\infty}^{\infty} c(t)(x(t)+e(t))e^{-j\pi\hat{k}t^2}e^{-jwt}dt$. $N(w)$ firstly performs nonlinear transformation on the useful communication signal and $S\alpha S$ noise, and then performs Fourier transform on the useful communication signal and $S\alpha S$ noise, in addition, $w = 2\pi f$, so we can obtain

$$\begin{aligned} GF(2\pi f) &\approx A\left(\frac{\log_e(|x(t)+A|)^{\frac{1}{e}}+1}{|x(t)+A|}\right)\delta(2\pi f - 2\pi f_0) \\ &\quad + N(2\pi f) \end{aligned} \tag{19}$$

The LFM signal is converted from the time domain to the frequency domain by GFT, and the $r_1(t)$ signal is a pulse signal, so the initial frequency $\hat{f}_0$ can be estimated by using the position of the maximum value as

$$\hat{f}_0 = \arg\max_f[GF(w)]\cdot\frac{\Delta f_1}{2\pi}, \tag{20}$$

where Δf_1 is sampling interval in the frequency domain of the GFT.

The procedure of the initial frequency estimation for LFM interference in $S\alpha S$ noise is summarized in Algorithm 2.

Algorithm 2 The initial frequency estimation for LFM interference in $S\alpha S$ noise

Input: $r(t)$: the received signal; $\hat{k}$: the estimated value of the chirp rate.

Output: $\hat{f}_0$: the estimated value of the initial frequency.

1: Constructed the demodulation reference signal $e^{-j\pi\hat{k}t^2}$ by the chirp rate $\hat{k}$, and then multiplied by the received signal $r(t)$ to obtain $r_1(t)$ by (15);
2: Obtain the GFT of $r_1(t)$ by (16);
3: Estimate the initial frequency $\hat{f}_0$ according to the position corresponding to the maximum value of $GF(w)$ by $\hat{f}_0 = \arg\max_f [GF(w)] \cdot \Delta f_1/2\pi$.

IV. Asymptotic Analysis of the Proposed Estimation Methods

A. Asymptotic Analysis of the Chirp Rate Estimation Method

According to the discussion in Section III, we obtain the estimation of the chirp rate by GELCT and Radon transform. In this section, we analyze the asymptotic property of the chirp rate estimation method. The asymptotic analysis of the chirp rate estimation can be considered as a asymptotic analysis of the generalized linear chirplet transform estimator $\hat{G}(t,w)$.

The estimator $\hat{G}(t,w)$ is expressed as

$$\hat{G}(t,w) = \frac{1}{N}\sum_{n=0}^{N-1} f\left[r(n)\right]h(n-t)e^{-jwn}e^{-j\frac{1}{2}(n-t)^2\frac{f_s}{2T_s}\tan\vartheta}, \tag{21}$$

and the mean value of $\hat{G}(t,w)$ is

$$\begin{aligned} &E\left(\hat{G}(t,w)\right)\\ =&E\left(\frac{1}{N}\sum_{n=0}^{N-1} f\left[r(n)\right]h(n-t)e^{-jwn}e^{-j\frac{1}{2}(n-t)^2\frac{f_s}{2T_s}\tan\vartheta}\right)\\ =&\frac{1}{N}\sum_{n=0}^{N-1} E\left(f\left[r(n)\right]h(n-t)e^{-jwn}e^{-j\frac{1}{2}(n-t)^2\frac{f_s}{2T_s}\tan\vartheta}\right). \end{aligned} \tag{22}$$

When $N\to\infty$, it can be derived that

$$\lim_{N\to\infty} E\left(\hat{G}(t,w)\right) = G(t,w). \tag{23}$$

Thus, the proposed estimator is asymptotically unbiased.

The mean square of $\hat{G}(t,w)$ can be expressed as

$$\begin{aligned} &E\left(\hat{G}^2(t,w)\right)\\ =&E\left(\left(\frac{1}{N}\sum_{n=0}^{N-1} f[r(n)]h(n-t)\right.\right.\\ &\left.\left.\cdot\ e^{-jwn}e^{-j\frac{1}{2}(n-t)^2\frac{f_s}{2T_s}\tan\vartheta}\right)^2\right)\\ =&\frac{1}{N^2}E\left(\left(\sum_{n=0}^{N-1} f[r(n)]h(n-t)\right.\right.\\ &\left.\left.\cdot\ e^{-jwn}e^{-j\frac{1}{2}(n-t)^2\frac{f_s}{2T_s}\tan\vartheta}\right)^2\right). \end{aligned} \tag{24}$$

When $N\to\infty$, it can be derived that

$$\begin{aligned} &\lim_{N\to\infty}\operatorname{var}\left[\hat{G}(t,w)\right]\\ =&\lim_{N\to\infty}\left(E(\hat{G}^2(t,w)) - E^2(\hat{G}(t,w))\right)\\ =&\lim_{N\to\infty}\left(E(\hat{G}^2(t,w))\right) - \lim_{N\to\infty}\left(E^2(\hat{G}(t,w))\right)\\ =&G^2(t,w) - G^2(t,w)\\ =&0. \end{aligned} \tag{25}$$

Thus, the proposed estimator is consistent.

B. Asymptotic Analysis of the Initial Frequency Estimation Method

According to the discussion in Section III, we get the estimation of the initial frequency by GFT. In this section, we analyze the asymptotic property of the initial frequency estimation method. The asymptotic analysis of the initial frequency estimate can be considered as a asymptotic analysis of the generalized Fourier transform estimator $\widehat{GF}(w)$.

The proposed estimator $\widehat{GF}(w)$ is expressed as

$$\widehat{GF}(w) = \frac{1}{N}\sum_{n=0}^{N-1} f[r_1(n)]\cdot e^{-jwn}, \tag{26}$$

and the mean value of $\widehat{GF}(w)$ is

$$E\left(\widehat{GF}(w)\right) = \frac{1}{N}\sum_{n=0}^{N-1} E\left(f[r_1(n)]\cdot e^{-jwn}\right). \tag{27}$$

When $N\to\infty$, we obtain

$$\lim_{N\to\infty} E\left(\widehat{GF}(w)\right) = GF(w). \tag{28}$$

Thus, the proposed estimator is asymptotically unbiased.

The mean square of $\widehat{GF}(w)$ can be expressed as

$$\begin{aligned} E(\widehat{GF}^2(w)) &= E\left(\left(\frac{1}{N}\sum_{n=0}^{N-1}(f[r_1(n)])\cdot e^{-jwn}\right)^2\right)\\ &= \frac{1}{N^2}E\left(\left(\sum_{n=0}^{N-1}(f[r_1(n)])\cdot e^{-jwn}\right)^2\right). \end{aligned} \tag{29}$$

When $N\to\infty$, we obtain

$$\begin{aligned} &\lim_{N\to\infty}\operatorname{var}\left[\widehat{GF}(w)\right]\\ =&\lim_{N\to\infty}\left(E(\widehat{GF}^2(w)) - E^2(\widehat{GF}(w))\right)\\ =&\lim_{N\to\infty}\left(E(\widehat{GF}^2(w))\right) - \lim_{N\to\infty}\left(E^2(\widehat{GF}(w))\right)\\ =&GF^2(w) - GF^2(w)\\ =&0. \end{aligned} \tag{30}$$

Thus, the proposed estimator is consistent.

V. CRLBs of Modulation Parameters Estimators

From the alpha-stable noise model described in this paper, we can see that there is no closed form of P.D.F. for the alpha-stable noise. When the value of α is 1 or 2, we can obtain two special distributions respectively, as Cauchy distribution ($\alpha = 1$) and Gauss distribution ($\alpha = 2$). For the Cauchy distribution, the P.D.F. is expressed as

$$f_1(\gamma,\delta;x) = \frac{1}{\pi}\frac{\gamma}{\gamma^2+(x-\delta)^2}, \tag{31}$$

where δ is the location parameter and γ is the dispersion parameter. For the Gauss distribution, the P.D.F. is be expressed as

$$f_2(\gamma,\delta;x) = \frac{1}{\sqrt{4\pi\gamma}}\exp\left[-\frac{(x-\delta)^2}{4\gamma}\right]. \tag{32}$$

This paper adopts the $S\alpha S$ distribution with location parameter $\delta = 0$ and dispersion parameter $\gamma = 1$. Then, the density function of the $S\alpha S$ distribution is expressed as $f(x)$, which is described in [22] and [23] as

$$f(x) = \begin{cases} \frac{1}{\pi x}\sum\limits_{k=1}^{\infty}\frac{(-1)^{k-1}}{k!}\Gamma(\alpha k+1)x^{-\alpha k}\sin(\frac{k\alpha\pi}{2}), \\ 0<\alpha<1, \\ \frac{1}{\pi(x^2+1)}, \alpha = 1, \\ \frac{1}{\pi\alpha}\sum\limits_{k=0}^{\infty}\frac{(-1)^k}{2k!}\Gamma(\frac{2k+1}{\alpha})x^{2k}, 1<\alpha<2, \\ \frac{1}{2\sqrt{\pi}}\exp[-\frac{x^2}{4}], \alpha = 2. \end{cases} \tag{33}$$

According to the LFM interference model and the alpha-stable noise model described in (1) and (2), a sampled discrete LFM interference and alpha-stable noise can be written as

$$\begin{aligned} &s(nT_s)+\mathrm{e}(nT_s) \\ =&A\cos(2\pi f_0 nT_s + k\pi(nT_s)^2) \\ +&jA\sin(2\pi f_0 nT_s + k\pi(nT_s)^2)+\mathrm{e}(nT_s), \end{aligned} \tag{34}$$

where $n = 0, ...N-1$.

Let the estimated vector be $\theta = [f_0, k]$. Then, the log-likelihood function of the estimated vector θ is expressed as follows [24]

$$\Lambda(r,\theta) = \sum_{n=0}^{N-1}[\ln f(e_{n,R}) + \ln f(e_{n,I})], \tag{35}$$

where $e_{n,R}$ is the real part of $e(nT_s)$ and $e_{n,I}$ is the imaginary part of $e(nT_s)$. Then the Fisher information matrix can be expressed as

$$\begin{aligned} &[I(\theta)]_{i,j} \\ =&-E\left\{\left[\frac{\partial\Lambda(r,\theta)}{\partial\theta_i}\right]\left[\frac{\partial\Lambda(r,\theta)}{\partial\theta_j}\right]^T\right\} \\ =&\sum_{\mathrm{n}=0}^{N-1}\left\{\frac{\partial s_{n,R}}{\partial\theta_i}\frac{\partial s_{n,R}}{\partial\theta_j}E[g'(e_{n,R})]+\frac{\partial s_{n,I}}{\partial\theta_i}\frac{\partial s_{n,I}}{\partial\theta_j}E[g'(e_{n,I})]\right\} \\ -&\sum_{\mathrm{n}=0}^{N-1}\left\{\frac{\partial^2 s_{n,R}}{\partial\theta_i\partial\theta_j}E[g(e_{n,R})]+\frac{\partial^2 s_{n,I}}{\partial\theta_i\partial\theta_j}E[g(e_{n,I})]\right\}, \end{aligned} \tag{36}$$

where $g(x) = \frac{-f'(x)}{f(x)}$, $s_{n,R}$ is the real part of $s(nT_s)$, and $s_{n,I}$ is the imaginary part of $s(nT_s)$,

$$\begin{aligned} E[g(e_{n,R})] &= \int_{-\infty}^{\infty} g(e_{n,R})f(e_{n,R})de_{n,R} \\ &= -[f(e_{n,R})]_{-\infty}^{\infty} = 0, \end{aligned} \tag{37}$$

and

$$\begin{aligned} E[g'(e_{n,R})] &= \int_{-\infty}^{\infty} g'(e_{n,R})f(e_{n,R})de_{n,R} \\ &= \int_{-\infty}^{\infty}[f'(e_{n,R})]^2/f(e_{n,R})de_{n,R}. \end{aligned} \tag{38}$$

Let $\int_{-\infty}^{\infty}[f'(e_{n,R})]^2/f(e_{n,R})de_{n,R}=\kappa(\alpha)$, then

$$E[g(e_{n,I})] = 0 \tag{39}$$

and

$$E[g'(e_{n,I})]=\int_{-\infty}^{\infty}[f'(e_{n,I})]^2/f(e_{n,I})de_{n,I} = \kappa(\alpha). \tag{40}$$

So (36) can be simplified as

$$[I(\theta)]_{i,j} = \kappa(\alpha)\sum_{\mathrm{n}=0}^{N-1}[\frac{\partial s_{n,R}}{\partial\theta_i}\frac{\partial s_{n,R}}{\partial\theta_j}+\frac{\partial s_{n,I}}{\partial\theta_i}\frac{\partial s_{n,I}}{\partial\theta_j}]. \tag{41}$$

Substituting (34) into (41), we obtain

$$[I(\theta)]_{1,1}=\kappa(\alpha)4A^2\pi^2T_s^2\sum_{n=0}^{N-1}n^2, \tag{42}$$

and

$$[I(\theta)]_{2,2}=\kappa(\alpha)A^2\pi^2T_s^4\sum_{n=0}^{N-1}n^4. \tag{43}$$

It can be obtained that the CRLBs of initial frequency and chirp rate, respectively, can be expressed as

$$\begin{aligned} CRLB(f_0) &= [I^{-1}(\theta)]_{1,1} \\ &= \frac{1}{4\kappa(\alpha)GSNR\pi^2T_s^2\sum\limits_{n=0}^{N-1}n^2} \\ &= \frac{6}{4\kappa(\alpha)GSNR\pi^2T_s^2\,(2N^3+3N^2+N)}, \end{aligned} \tag{44}$$

and

$$\begin{aligned} CRLB(\mathrm{k}) &= [I^{-1}(\theta)]_{2,2} \\ &= \frac{1}{\kappa(\alpha)GSNR\pi^2T_s^4\sum\limits_{n=0}^{N-1}n^4} \\ &= \frac{30}{\kappa(\alpha)GSNR\pi^2T_s^4\,(6N^5+15N^4+10N^3)}. \end{aligned} \tag{45}$$

When $\alpha = 1$, the $S\alpha S$ distribution is Cauchy, and

$$\begin{aligned} \kappa(\alpha) &= \int_{-\infty}^{\infty}\left(\left(\left(\frac{1}{\pi(x^2+1)}\right)'\right)^2\Big/\frac{1}{\pi(x^2+1)}\right)dx \\ &= \int_{-\infty}^{\infty}\frac{(2\pi x)^2}{(\pi\,(x^2+1))^3}dx \\ &= \frac{1}{2}. \end{aligned} \tag{46}$$

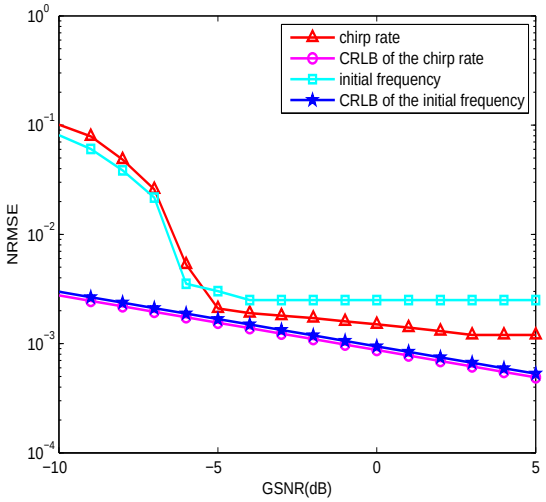

Fig. 1. Estimation performance of the chirp rate and the initial frequency with $\alpha = 1$.

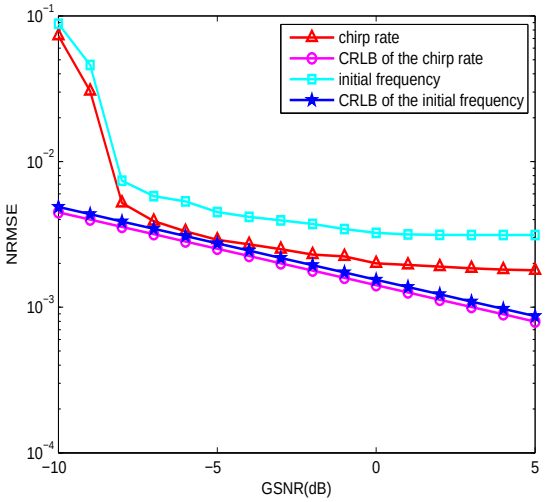

Fig. 2. Estimation performance of the chirp rate and the initial frequency with $\alpha = 2$.

Therefore, the corresponding CRLBs can be expressed as

$$CRLB(f_0)=\frac{6}{2GSNR\pi^2T_s^2\left(2N^3+3N^2+N\right)}, \tag{47}$$

and

$$CRLB(\mathrm{k}) = \frac{60}{GSNR\pi^2T_s^4\left(6N^5+15N^4+10N^3\right)}. \tag{48}$$

When $\alpha = 2$, the $S\alpha S$ distribution is Gaussian, and

$$\begin{aligned}&\kappa(\alpha)\\ &=\int_{-\infty}^{\infty}\left(\left(\left(\frac{1}{2\sqrt{\pi}}\exp[-\frac{x^2}{4}]\right)'\right)^2\Big/\frac{1}{2\sqrt{\pi}}\exp[-\frac{x^2}{4}]\right)dx\\ &=\int_{-\infty}^{\infty}\left(\frac{1}{2\sqrt{\pi}}\cdot\frac{x^2}{4}\cdot\exp[-\frac{x^2}{4}]\right)dx\\ &=2.\end{aligned} \tag{49}$$

Therefore, the corresponding CRLBs can be expressed as

$$CRLB(f_0)=\frac{3}{4GSNR\pi^2T_s^2\left(2N^3+3N^2+N\right)}, \tag{50}$$

and

$$CRLB(\mathrm{k}) = \frac{15}{GSNR\pi^2T_s^4\left(6N^5+15N^4+10N^3\right)}. \tag{51}$$

VI. Numerical Results and Discussion

In order to evaluate the performance of the proposed method, MATLAB simulation is carried out. In this paper, the parameter setups of LFM interference in DSSS communication systems are described as follows: the initial frequency is f_0 = 1000Hz, the chirp rate is k = 10000Hz/s, the data length is 1024 points, the sampling frequency is f_s = 10240Hz, and the signal duration is T_s = 0.1s. The noise is the standard additive $S\alpha S$ noise. The parameter estimation performance is

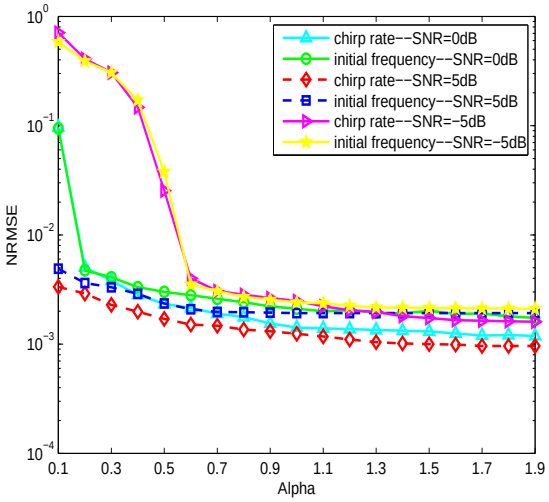

Fig. 3. Estimation performance of the chirp rate and the initial frequency with different characteristic exponents.

measured by the normalized root mean square error (NRMSE), which is defined as

$$NRMSE = 10\lg\sqrt{\sum_{i=1}^{N}\left(Y-\hat{Y}(i)\right)^2/\left(N\cdot Y^2\right)}, \tag{52}$$

where N is the number of Monte Carlo simulation experiments, and the value of N in this paper is 3000. The actual value of the parameter Y to be estimated is $\hat{Y}(i)$.

Here, the estimation performance of the chirp rate and the initial frequency is assessed. Let the characteristic exponents be $\alpha = 1$ and $\alpha = 2$, respectively. Fig. 1 presents the estimation performance of the proposed method for $\alpha = 1$. From Fig. 1, we observe that, when the GSNR is -5dB, the NRMSE of the chirp rate approaches 0.2×10^{-2}. In addition, the NRMSE of the initial frequency approaches 0.3×10^{-2} when the GSNR is -6dB. The chirp rate and the initial

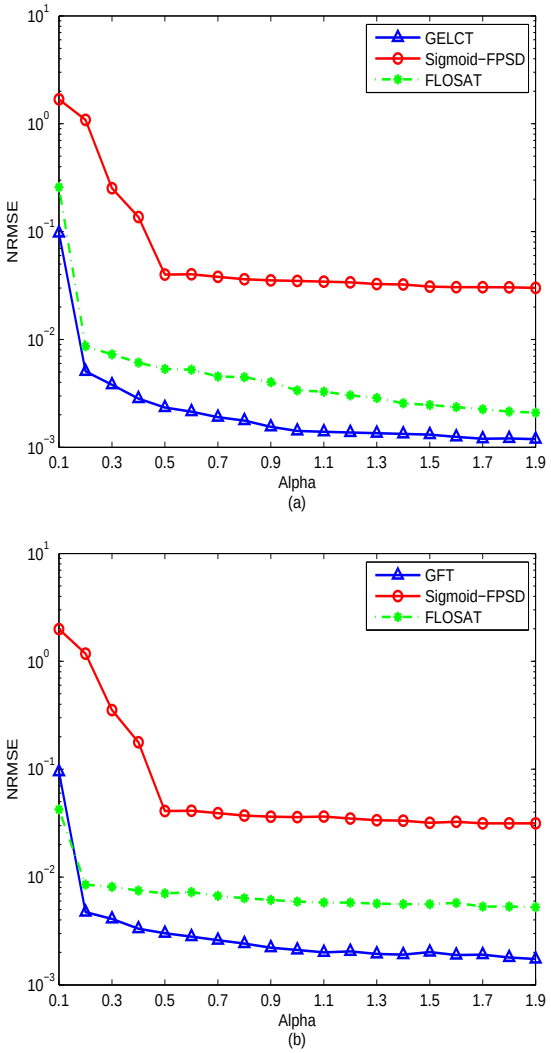

Fig. 4. (a) Performance comparison of the chirp rate estimation with different characteristic exponents and $GSNR = 0dB$ (b) Performance comparison of the initial frequency estimation with different characteristic exponents and $GSNR = 0dB$.

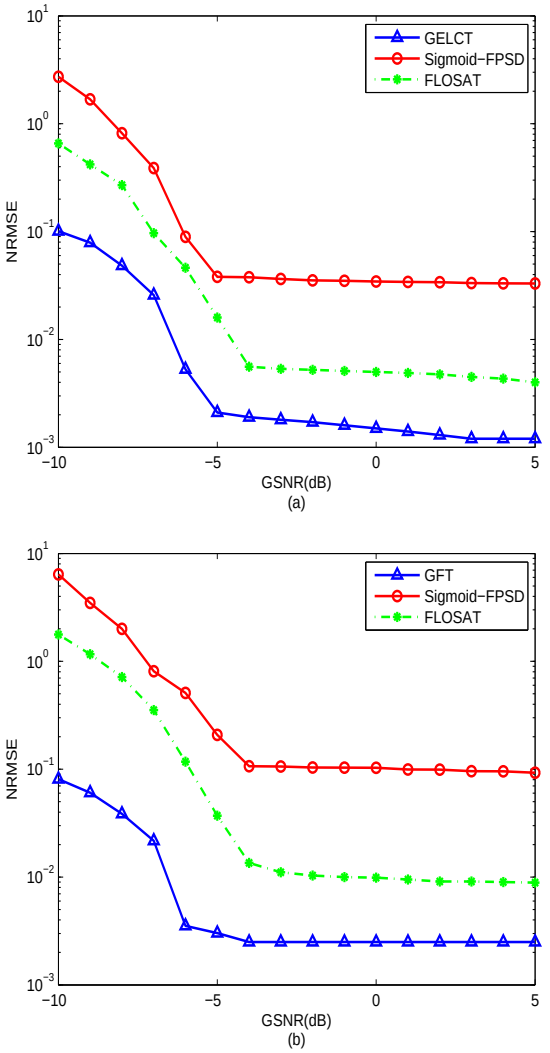

Fig. 5. (a) Performance comparison of the chirp rate estimation with different $GSNRs$ and $\alpha = 1$ (b) Performance comparison of the initial frequency estimation with different $GSNRs$ and $\alpha = 1$.

frequency curves are close to the CRLBs, implying that the proposed estimation method is effective and feasible. When $\alpha = 2$, the estimation performance of the proposed method is shown in Fig. 2. It is seen that the NRMSE of the chirp rate is close to 0.2×10^{-2} and the NRMSE of the initial frequency is close to 0.3×10^{-2}, when the GSNR is -8dB. Furthermore, both the chirp rate and the initial frequency estimation curves of the proposed method approach their CRLBs. It is evident that the proposed method is also feasible in Gaussian noise environment.

In Fig. 3, the estimation performance of the chirp rate and the initial frequency with different characteristic exponents α are evaluated. Moreover, the estimation performance of the proposed method is demonstrated. From Fig. 3, under the condition that the GSNR is -5dB and the characteristic exponent is greater than 0.6, the estimation performance is stable. Also, the stability of the estimation performance is guaranteed, when the GSNR and the characteristic exponent are 0dB and greater than 0.2, respectively. Another important observation is that the estimation performance of the chirp rate and the initial frequency is not affected by the characteristic exponent when the GSNR is higher than 5dB, indicating that the proposed estimation method is robust to the characteristic exponent in the high GSNR regime.

Under the same simulation environments and parameter settings, the performance of the proposed method is compared with the methods introduced in [13] and [14]. In [13], the fractional Fourier transform and Sigmoid transform (Sigmoid-FPSD) are used to estimate the chirp rate and the initial frequency of the LFM interference. The authors in [14] proposed a method based on fractional low-order statistic and scaling ambiguity transform (FLOSAT) to estimate the chirp rate and the initial frequency of the LFM interference. Fig. 4 shows the estimation performance of the proposed method compared with referred methods under different characteristic exponents and GSNR = 0dB. From Fig. 4, it is clear that the NRMSE of this method is reduced by 0.028 compared with the Sigmoid-

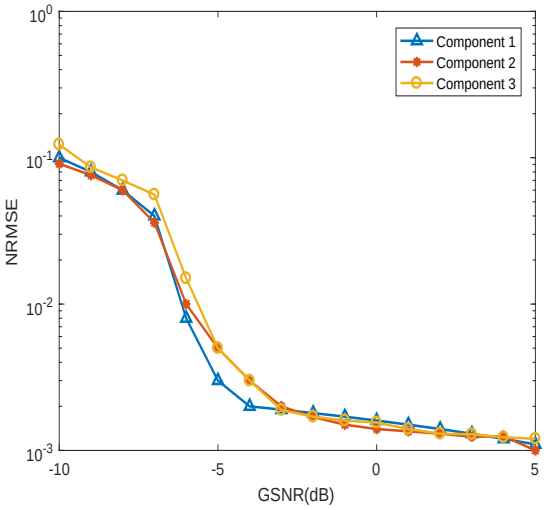

Fig. 6. Chirp rate estimation performance of multi-component LFM interference.

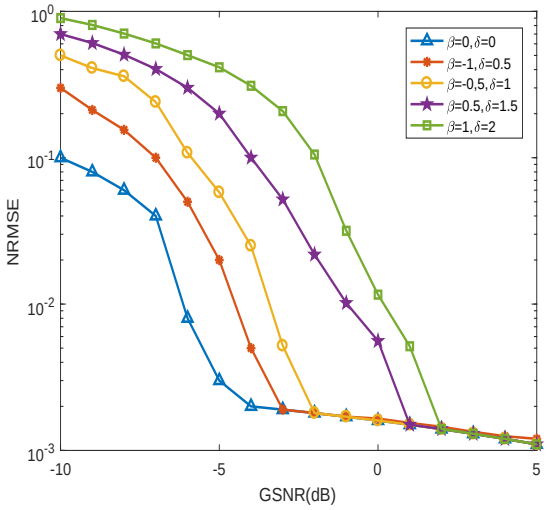

Fig. 8. Chirp rate estimation performance of LFM in general alpha-stable noise.

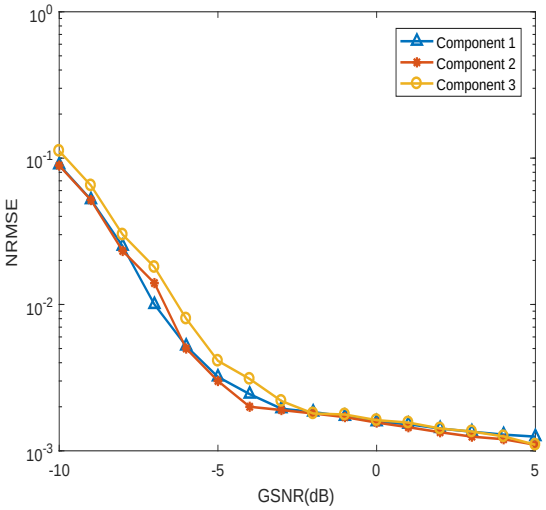

Fig. 7. Initial frequency estimation performance of multi-component LFM interference.

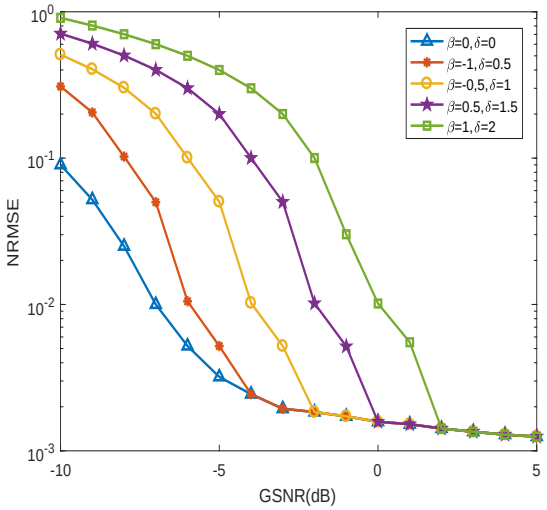

Fig. 9. Initial frequency estimation performance of LFM in general alpha-stable noise.

FPSD method proposed in [13], and the NRMSE is reduced by 0.003 compared with the FLOSAT method proposed in [14]. Fig. 5 illustrates the estimation performance of the proposed method compared with those of the methods in [13] and [14] under different GSNRs and $\alpha = 1$. The proposed method has better estimation performance than the existing methods. From Fig. 5, it is clear that the NRMSE of the proposed method is reduced by 0.098 compared with the Sigmoid-FPSD method proposed in [13], and the NRMSE is reduced by 0.008 compared with the FLOSAT method proposed in [14]. The computational complexity of the proposed method, the method in [13], and the method in [14] can be expressed by $O\left(2N^2\log_2 N\right)$, $O\left(2N^2\log_2 N\right)$, and $O\left(N^3\log_2 N\right)$, respectively. The comparison of the computational complexity indicates that the computational complexity of the proposed method is significantly lower than that of the method in [14] method, and is almost same as that of the method in [13].

The proposed parameter estimation method in this paper is also applicable to multi-component LFM interference. The chirp rate and the initial frequency of each LFM interference signal are set as $k_1 = 1 \times 10^4, f_{01} = 1 \times 10^3$, $k_2 = 2 \times 10^4, f_{02} = 2 \times 10^3$ and $k_3 = 3 \times 10^4, f_{03} = 3 \times 10^3$, respectively. Fig. 6 shows the estimation performance of the chirp rate of the multi-component LFM interference. Fig. 7 shows the estimation performance of the initial frequency of a multi-component LFM interference. From Fig. 6 and Fig. 7, it can be seen that the parameters estimation of the proposed method for three-component LFM interference is effective and feasible. In particular, when the chirp rate or the initial frequency of the three-component LFM interference signal is the same, the estimation performance of the corresponding initial frequencies or the chirp rates are slightly different at low GSNR, and the estimation performance are gradually the same as the GSNR increase.

The parameter estimation algorithm proposed in this paper is also applicable to LFM interference parameter estimation in general alpha-stable noise. Fig. 8 and Fig. 9 are the estimation performance of the LFM interference signal the chirp rate and the initial frequency with $\beta = 0, -1, -0.5, 0.5, 1$ and $\delta = 0, 0.5, 1, 1.5, 2$, respectively. From Fig. 8 and Fig. 9, we can be seen that the LFM interference parameter estimation performance gradually decrease as the β and δ change and the estimation performance in the symmetric alpha-stable noise is the best.

VII. Conclusion

This paper introduces a novel modulation parameter estimation method of LFM interference for DSSS communication systems in alpha-stable noise. The proposed method is asymptotically consistent, and the CRLBs of the modulation parameter estimation is analyzed for the variance of the unbiased estimator. Simulation results and theoretical analysis show that this method can not only effectively suppress the impulse noise interference, but also has higher estimation accuracy and lower computational complexity in the alpha-stable noise environment compared with existing methods. Future work is to improve the method to make it has better estimation performance over fading channels.

Appendix A
Proof of Property 1

The nonlinear transformation of the received signal can be expressed as:

$$\begin{aligned} f[r(t)] =& f[x(t)+s(t)+e(t)] \\ =& \left(\frac{\log_e(|x(t)+s(t)+e(t)|)^{\frac{1}{e}}+1}{|x(t)+s(t)+e(t)|}\right) \\ & \cdot (x(t)+s(t)+e(t)). \end{aligned} \tag{53}$$

The proof of the nonlinear transformation in (8) is divided into the following three cases:

1) When the noise is low, that is $|x(t)+s(t)| \gg |e(t)|$. Assume $r(t) \approx x(t)+s(t) = x(t)+A\exp(j2\pi(f_0t+\frac{1}{2}kt^2))$, then

$$\begin{aligned} f[r(t)] \approx & \left(\frac{\log_e\left(\left|x(t)+A\exp(j2\pi(f_0t+\frac{1}{2}kt^2))\right|\right)^{\frac{1}{e}}+1}{\left|x(t)+A\exp(j2\pi(f_0t+\frac{1}{2}kt^2))\right|}\right) \\ & \cdot (x(t)+A\exp(j2\pi(f_0t+\frac{1}{2}kt^2))) \\ \approx & \left(\frac{\frac{1}{e}\log_e(|A|+|x(t)|)+1}{(|A|+|x(t)|)}\right) \\ & \cdot (x(t)+A\exp(j2\pi(f_0t+\frac{1}{2}kt^2))) \end{aligned} \tag{54}$$

2) When the noise is high, the main performance of $S\alpha S$ noise is a short-time large-scale pulse, which is also the main interference of $S\alpha S$ noise on the useful signal, that is $|x(t)+s(t)| \ll |e(t)|$. Therefore, this can be approximated as $r(t) \approx e(t)$. Then

$$\begin{aligned} f[r(t)] &\approx \left(\frac{\log_e(|e(t)|)^{\frac{1}{e}}+1}{|e(t)|}\right) e(t) \\ &\approx \frac{1}{e}\log_e|e(t)|+1. \end{aligned} \tag{55}$$

3) When $|x(t)+s(t)| \approx |e(t)|$,

$$\begin{aligned} f[r(t)] &= f[x(t)+s(t)+e(t)] \\ &= \left(\frac{\log_e(|x(t)+s(t)+e(t)|)^{\frac{1}{e}}+1}{|x(t)+s(t)+e(t)|}\right) \\ &\cdot (x(t)+s(t)+e(t)) \\ &= c(t)\,(x(t)+s(t)+e(t)) \\ &= x_0(t)+s_0(t)+e_0(t), \end{aligned} \tag{56}$$

where $c(t)$ is real numbers, and $c(t)=\frac{\log_e(|x(t)+s(t)+e(t)|)^{\frac{1}{e}}+1}{|x(t)+s(t)+e(t)|}$. $x(t)$, $s(t)$ and $e(t)$ are independent of each other, so $x_0(t) = x(t)c(t)$, $s_0(t) = s(t)c(t)$ and $e_0(t) = e(t)c(t)$ are also independent of each other. $s_0(t)$ and $s(t)$ are only the difference in amplitude, and the phase has not changed.

Appendix B
Proof of Property 2

GFT performs a nonlinear transformation on the signal to suppress $S\alpha S$ noise and retain useful signal information. The nonlinear transformation on $r_1(t)$ is expressed as

$$\begin{aligned} & f[r_1(t)] \\ =& f[Ae^{j2\pi f_0t}+(e(t)+x(t))\cdot e^{-j\pi\hat{k}t^2}] \\ =& \left(\frac{\log_e(\left|Ae^{j2\pi f_0t}+(e(t)+x(t))\cdot e^{-j\pi\hat{k}t^2}\right|)^{\frac{1}{e}}+1}{\left|Ae^{j2\pi f_0t}+(e(t)+x(t))\cdot e^{-j\pi\hat{k}t^2}\right|}\right) \\ & \cdot \left(Ae^{j2\pi f_0t}+(e(t)+x(t))\cdot e^{-j\pi\hat{k}t^2}\right) \\ =& \left(\frac{\log_e(|x(t)+A+e(t)|)^{\frac{1}{e}}+1}{|x(t)+A+e(t)|}\right) \\ & \cdot \left(Ae^{j2\pi f_0t}+(x(t)+e(t))e^{-j\pi\hat{k}t^2}\right) \\ =& c(t)\left(Ae^{j2\pi f_0t}+(x(t)+e(t))\cdot e^{-j\pi\hat{k}t^2}\right) \\ =& c(t)\cdot Ae^{j2\pi f_0t}+c(t)\cdot(x(t)+e(t))\cdot e^{-j\pi\hat{k}t^2} \\ =& x_1(t)+s_1(t)+e_1(t) \end{aligned} \tag{57}$$

where $c(t)=\frac{\log_e(|x(t)+A+e(t)|)^{\frac{1}{e}}+1}{|x(t)+A+e(t)|}$ is a real number, $x_1(t) = c(t)\cdot x(t)\cdot e^{-j\pi\hat{k}t^2}$, $s_1(t) = c(t)\cdot Ae^{j2\pi f_0t}$, and $e_1(t) = c(t)\cdot e(t)\cdot e^{-j\pi\hat{k}t^2}$. $x(t)\cdot e^{-j\pi\hat{k}t^2}$, $Ae^{j2\pi f_0t}$ and $e(t)\cdot e^{-j\pi\hat{k}t^2}$ are independent of each other, so $x_1(t)$, $s_1(t)$ and $e_1(t)$ are also independent of each other. $s_1(t)$ and $Ae^{j2\pi f_0t}$ only the differ in amplitude, and the phases are the same.

REFERENCES

[1] S. Liu, T. Shan, Y. Zhang, R. Tao and Y. Feng, "A fast algorithm for multi-component LFM signal analysis exploiting segmented DPT and SDFrFT," in *Proc. 2015 IEEE Radar Conference*, Arlington, VA, USA, May 2015, pp. 1-4.

[2] G. Fu, J. Lin, Q. He, "The application of a linear FM interference suppression in DSSS technology systems," *Applied Mechanics and Materials*, vol. 3468, no. 1294, pp. 4599-4602, July. 2014.

[3] Y. Jiang, S. Yin and O. Kaynak, "Data-driven monitoring and safety control of industrial cyber-physical systems: basics and beyond," *IEEE Access*, vol. 6, pp. 47374-47384, Aug. 2018.

[4] Y. Zhang, X. Jia and W. Zhu, "Suppression of LFM interference in direct sequence spread spectrum communications based on compressive sensing," in *Proc. 2015 IEEE International Conference on Signal Processing, Communications and Computing*, Ningbo, China, Sept. 2015, pp. 1-5.

[5] X. Qiao, J. Qian and T. Liang, "Suppression of LFM inteference for DSSS communication system based on FRFT," in *Proc. 2011 International Conference on Electronics, Communications and Control*, Ningbo, China, Sept. 2011, pp. 1-4.

[6] H. Song, X. Fang, and Y. Fang, "Unlicensed spectra fusion and interference coordination for LTE systems," *IEEE Transactions on Mobile Computing*, vol. 15, no. 12, pp. 3171-3184, Dec. 2016.

[7] H. Song, X. Fang, and C. Wang, "Cost-reliability tradeoff in licensed and unlicensed spectra interoperable networks with guaranteed user data rate requirements," *IEEE Journal on Selected Areas in Communications*, vol. 35, no. 1, pp. 200-214, Jan. 2017.

[8] Z. Qiu, J. Zhu and F. Li, "Multiple BPSK/LFM hybrid modulated signals parameter estimation and analysis intercepted by non-cooperative radar receiver," in *Proc. 2018 IEEE International Conference on Computational Electromagnetics*, Chengdu, China, Oct. 2018, pp. 1-4.

[9] K. Ding, Q. Ding and R. Lan, "Parameters estimation of LFM signal based on fractional order cross spectrum," in *Proc. 2011 International Conference on Mechanical Engineering and Information Technology*, Harbin, China, Aug. 2011, pp. 654-656.

[10] S. Pei and S. Huang, "STFT with adaptive window width based on the chirp rate," *IEEE Transactions on Signal Processing*, vol. 60, no. 8, pp. 4065-4080, Aug. 2012.

[11] Q. Chen, Y. Li, and M. Zhu, "Fast algorithm for parameter estimation of LFM signals under low SNR," in *Proc. AIP Conference Proceedings*, vol. 1839, no. 1, pp. 1-7, May 2017.

[12] P. Zhang, P. Wang and J. Cheng, "Time-domain approach for LFM signal parameter estimation based on FPGA," *Electronics Letters*, vol. 54, no. 13, pp. 846-848, June 2018.

[13] L. Li and T. Qiu, "A robust parameter estimation of LFM signal based on sigmoid transform under the alpha stable distribution noise," *Circuits, Systems, and Signal Processing*, vol. 38, no. 7, pp. 3170-3186, Jan. 2019.

[14] Y. Jin, P. Duan and H. Ji, "Parameter estimation of LFM signals based on scaled ambiguity function," *Circuits, Systems, and Signal Processing*, vol. 35, no. 12, pp. 4445-4462, Mar. 2016.

[15] G. Gu, Y. Zhang and B. Tian, "Estimation of LFM signal's time parameters under the alpha-stable distribution noise," in *Proc. 2009 IEEE Circuits and Systems International Conference on Testing and Diagnosis*, Chengdu, China, Apr. 2009, pp. 1-4.

[16] Q. Meng, G. Shao and B. Wang, "Identification and parameter estimation of underwater LFM signals under alpha-Stable distribution noise," in *Proc. IEEE International Conference on Electronics Information and Emergency Communication*, Beijing, China, June 2018, pp. 190-193.

[17] M. Liu, N. Zhao, J. Li and V. Leung, "Spectrum sensing based on maximum generalized correntropy under symmetric alpha stable noise," *IEEE Transactions on Vehicular Technology*, vol. 68, no. 10, pp. 10262-10266, Oct. 2019.

[18] Y. Guan, M. Liang and D. Necsulescu, "Velocity synchronous linear Chirplet transform," *IEEE Transactions on Industrial Electronics*, vol. 66, no. 8, pp. 6270-6280, Aug. 2019.

[19] Y. Miao, H. Sun and J. Qi, "Synchro-compensating Chirplet transform," *IEEE Signal Processing Letters*, vol. 25, no. 9, pp. 1413-1417, Sept. 2018.

[20] F. Shen, L. Chen, G. Ding and Q. Wu, "Impact of nonlinear transformation on signal detection: A minimum error probability perspective," in *Proc. International Conference in Communications, Signal Processing, and Systems*, Harbin, China, July 2017, vol. 463, pp. 1583-1591.

[21] M. Mohammadi, A. Pouyan, N. Khan and V. Abolghasemi, "An improved design of adaptive directional time-frequency distributions based on the radon transform," *Signal Processing*, vol. 150, pp. 85-89, Sep. 2018.

[22] J. Zhang, N. Zhao, M. Liu, Y. Chen, H. Song, F. Gong, F. Yu, "Modified Cramer-rao bound for M-FSK signal parameter estimation in cauchy and gaussian noise," *IEEE Transactions on Vehicular Technology*, vol. 68, no. 10, pp. 10283-10288, Oct. 2019.

[23] M. Liu, J. Zhang, J. Tang, F. Jiang, P. Liu, F. Gong and N. Zhao, "2-D DOA robust estimation of echo signals based on multiple satellites passive radar in the presence of alpha stable distribution noise," *IEEE Access*, vol. 7, pp. 16032- 16042, Jan. 2019.

[24] J. Wang, B. Li, M. Liu, and J. Li, "SNR estimation of time-frequency overlapped signals for underlay cognitive radio," *IEEE Communications Letters*, vol. 19, no. 11, pp. 1925-1928, Nov. 2015.